

Strong Angular Momentum Effects in Near-Barrier Fusion Reactions

B. Haas, G. Duchêne, F. A. Beck, T. Byrski, C. Gehringer, J. C. Merdinger, A. Nourredine,
V. Rauch, and J. P. Vivien

Centre de Recherches Nucléaires, 67037 Strasbourg Cedex, France

and

J. Barrette and S. Tobbeche

*Département de Physique Nucléaire et Hautes Energies, Centre d'Etudes Nucléaire de Saclay,
91191 Gif sur Yvette Cedex, France*

and

E. Bożek and J. Styczen

Institute of Nuclear Physics Krakow, 30-342 Krakow, Poland

and

J. Keinonen

University of Helsinki, Accelerator Laboratory, SF-00550 Helsinki, Finland

and

J. Dudek

Centre de Recherches Nucléaires, 67037 Strasbourg Cedex, France

and

W. Nazarewicz

The Niels Bohr Institute, 2100 Copenhagen, Denmark

(Received 13 November 1984)

Cross sections and γ -ray multiplicities have been measured for neutron evaporation channels in the reactions $^{16}\text{O} + ^{144}\text{Nd}$, $^{37}\text{Cl} + ^{123}\text{Sb}$, $^{64}\text{Ni} + ^{96}\text{Zr}$, and $^{80}\text{Se} + ^{80}\text{Se}$ leading to the compound system ^{160}Er at common excitation energies. In the near-barrier energy regime average angular momentum transfers depend dramatically on the asymmetry of the entrance channel. The results are interpreted in terms of the ground-state zero-point vibrations.

PACS numbers: 25.70.Jj, 24.60.Dr

It is generally expected that compound nuclei formed at given excitation energies and angular momenta follow a "statistical" decay pattern independent of a particular reaction that led to fusion. Measurements of total-fusion cross sections and average γ multiplicities indeed confirmed such expectations in many cases. Successes of the classical-type description of the fusion cross section (e.g., Bass model¹) suggested that the maximum angular momentum transferred to the compound nucleus may be determined by the fusion cross section alone via the classical "sharp cut-off formula, independent of the reaction. Recently it has been discussed that in the near-barrier energy regime the simple picture does not apply anymore (cf. Broglia² and Dasso² and references therein), but our present knowledge of the underlying mechanisms comes mainly from studies of the total-fusion cross sections alone.

In this Letter we report for the first time on extensive data concerning the average transferred angular momentum as a function of the entrance-channel mass

asymmetry. For symmetric systems the transferred angular momentum is much larger than classical estimates and this influences considerably the individual evaporation-residue cross sections. The results are reproduced quantitatively after taking into account ion-ion potential-barrier fluctuations related to the ground-state shape vibrations.

We investigated the reactions $^{16}\text{O} + ^{144}\text{Nd}$, $^{37}\text{Cl} + ^{123}\text{Sb}$, $^{64}\text{Ni} + ^{96}\text{Zr}$, and $^{80}\text{Se} + ^{80}\text{Se}$ leading to the ^{160}Er compound system. (We used the Strasbourg 18 MV MP tandem facility.) In each reaction we produced ^{160}Er at excitation energies $E^* = 48.5, 53.5,$ and 58.5 MeV. The incident energies were adjusted, taking into account the energy loss in the enriched ~ 500 $\mu\text{g}/\text{cm}^2$ targets. The target thickness was determined by measurement of the cross section for Coulomb excitation of the first 2^+ state ($\frac{3}{2}^+$ in ^{123}Sb) by use of ^{16}O and ^{37}Cl beams at incident energies well below the Coulomb barrier and by Rutherford backscattering with use of 2 MeV ^4He particles from the University of Helsinki Van de Graaff accelerator. Results of both

TABLE I. Measured cross sections and average γ -ray multiplicities in the four reactions leading to the compound nucleus ^{160}Er at 48.5 MeV excitation energy.

	^{16}O		^{37}Cl		^{64}Ni		^{80}Se	
	σ (mb)	$\langle M_\gamma \rangle$	σ (mb)	$\langle M_\gamma \rangle$	σ (mb)	$\langle M_\gamma \rangle$	σ (mb)	$\langle M_\gamma \rangle$
2n	9(2)	16(2)	2(1)	17(4)	12(2)	26(3)	9(2)	27(2)
3n	225(8)	12(1)	28(2)	14(1)	46(8)	16(1)	50(11)	17(1)
4n	162(12)	10(1)	27(2)	10(1)	17(3)	12(1)	23(3)	12(1)
5n	3(1)	8(3)
ER ^a	399(52)		57(9)		75(16)		82(20)	

^aER is the sum of the individual 2-5 neutron exit channels.

methods agreed within 10%.

The evaporation cross sections are deduced from the absolute-intensity measurements of the γ rays emitted by the daughter nuclei. For the studied neutron-rich ^{160}Er compound nucleus, the evaporation of neutrons is the predominant decay mode. Therefore, by registering the last transitions in the various $^{158-155}\text{Er}$ channels³ one can determine not only individual cross sections but to a good approximation also the total evaporation-residue (ER) cross section. Singles γ spectra were recorded with two Ge detectors (18 and 120 cm³) positioned at $\pm 55^\circ$ to the beam axis. To measure average γ -ray multiplicities, $\langle M_\gamma \rangle$, the Ge detectors were used, each in coincidence with two lead-collimated 12.5×15.0 cm² NaI counters placed 35 cm from the target and at $\pm 125^\circ$ to the beam direction. By comparison of the coincidence-to-singles rates in the Ge detectors, $\langle M_\gamma \rangle$ values were extracted for the individual neutron-evaporation channels as

described by Ward *et al.*⁴

The measured absolute cross sections and the average γ -ray multiplicities are listed in Table I for the different reaction channels at $E^* = 48.5$ MeV. Similar results are obtained at the other energies. The present data confirm the enhancement of the two-neutron emission observed previously^{5,6} for fusion induced by heavy projectiles but indicate, furthermore, a strong effect of the entrance-channel asymmetry. For example, the ratio $R = \sigma(3n)/\sigma(2n)$ which is larger than 20 in the most asymmetric case is reduced to 5 in the symmetric reaction. This result may seem surprising since as indicated in Table II the average angular-momentum transfer, $\langle L_{\text{ER}} \rangle$, obtained from the total cross section in the sharp cutoff approximation are within experimental errors equal for the ^{16}O -, ^{64}Ni -, and ^{80}Se -induced reactions. (It has been suggested⁵ that such an enhancement in symmetric reactions may be due to trapping of the compound system in a super-

TABLE II. Average angular momenta L (\hbar), cross sections σ (mb), and ratios $R = [\sigma(3n)/\sigma(2n)]$ (see text). Energies E^* in megaelectronvolts.

E^*	$\langle L_{\text{ER}} \rangle$	$\langle L_\gamma \rangle$	$\langle L_\nu \rangle$	$\sigma_{\text{expt.}}$	$\sigma_{\text{calc.}}$	$R_{\text{expt.}}$	$R_{\text{calc.}}$
$^{16}\text{O} + ^{144}\text{Nd}$							
48.5	17(1)	18(1)	19	399(52)	485	25(6)	23
53.5	20(2)	23(2)	22	513(67)	669	25(5)	25
58.5	22(2)	27(2)	26	590(84)	838	> 38	45
$^{37}\text{Cl} + ^{123}\text{Sb}$							
48.5	14(2)	20(2)	20	57(9)	29	14(7)	15
53.5	20(2)	25(2)	25	125(18)	126	23(12)	18
58.5	24(2)	31(3)	30	197(28)	278	> 21	35
$^{64}\text{Ni} + ^{96}\text{Zr}$							
48.5	16(2)	30(3)	26	75(16)	92	3.8(0.9)	2.9
53.5	22(2)	32(3)	31	133(28)	200	4.5(1.1)	2.8
58.5	25(3)	37(3)	37	166(36)	329	5.9(1.6)	3.4
$^{80}\text{Se} + ^{80}\text{Se}$							
48.5	17(2)	29(3)	27	82(20)	84	5.6(1.8)	2.8
53.5	22(2)	31(3)	32	124(28)	182	3.3(0.9)	2.6
58.5	28(3)	37(3)	38	191(38)	317	4.6(1.3)	3.2

deformed potential well.) However, the measured γ -ray multiplicities lead to a different picture. To estimate the average entry spin $\langle I_\gamma \rangle$ for each reaction channel, we use the approximate relation⁷ $\langle I_\gamma \rangle = 2(\langle M_\gamma \rangle - 4) + I_0$ and $I_0 = 0$ or $\frac{13}{2}$ for $^{156,158}\text{Er}$ or $^{155,157}\text{Er}$, respectively. We neglect the angular momentum possibly removed by statistical transitions. The residual Er isotopes are known to be good rotors and therefore we assume that all other γ transitions are of the stretched $E2$ type. The total average angular

momentum $\langle L_\gamma \rangle$ is equal to $\sum_x \sigma_{(xn)} \langle I_\gamma \rangle_{xn} / \sum_x \sigma_{(xn)}$ (cf. Table II). For the most asymmetric entrance channel, the $\langle L_\gamma \rangle$ and $\langle L_{ER} \rangle$ values are comparable. However, in the symmetric or almost-symmetric cases $\langle L_\gamma \rangle$ is considerably larger than $\langle L_{ER} \rangle$. This large difference suggests that in symmetric reactions the observed enhancement of the $2n$ channel could be due to the properties of the entrance channel rather than to the properties of the decaying compound system.

To test this idea we have calculated the fusion

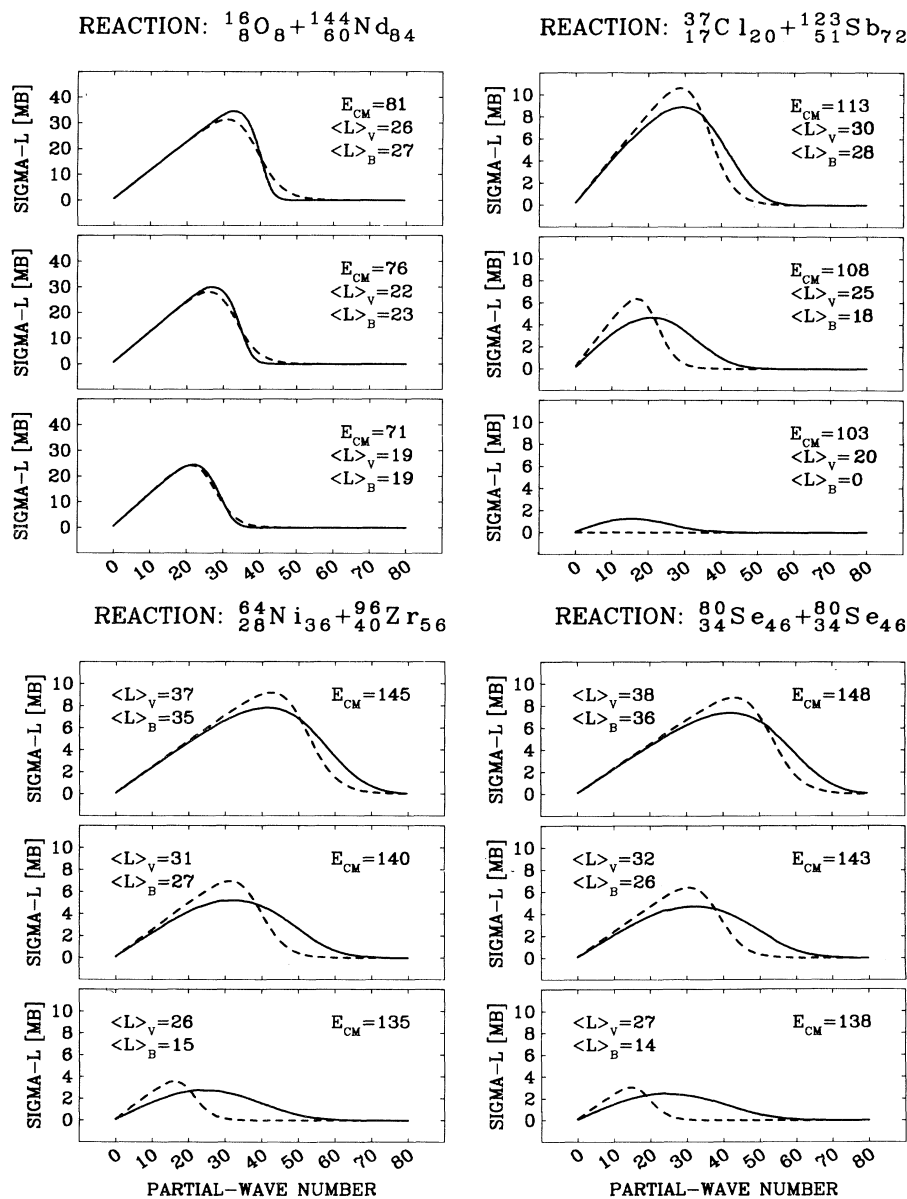


FIG. 1. Angular-momentum distributions calculated by taking into account ground-state vibrations. For comparison distributions (dashed line) and average values $\langle L \rangle_B$ calculated in the smooth cutoff Bass model are also shown. $E_{c.m.} = 103$ MeV corresponds to subbarrier fusion in the $^{37}\text{Cl} + ^{123}\text{Sb}$ reaction.

partial-wave distribution using the phenomenological ion-ion proximity potential of Blocki *et al.*⁸ Since the bombarding energies considered here are close to (or below) the Coulomb barrier we take into account the effect of the zero-point surface vibrations in both colliding ions. This mechanism discussed by Esbensen *et al.*⁹ and in Ref. 2 has been shown¹⁰ to represent a particular case of the more general coupled-channel approach.

The fusion probability in the partial wave l is calculated as

$$P_l(E_{c.m.}) = \int df_1 \int df_2 T_l(E_{c.m.}; f_1, f_2) P(f_1) P(f_2),$$

where T_l is the potential-barrier transmission coefficient and f_i denotes the actual deviation of the radius from its static (spherical) value $R_0^{(i)}$ ($i = 1$ for the projectile, and $i = 2$ for the target nuclei). Under simplifying assumptions the radius-deviation probability is given by a Gaussian distribution in which the variance σ is related to the surface oscillations by (see, e.g., Ref. 2)

$$\sigma^2 = R_0^2 \sum_n \sum_\lambda [(2\lambda + 1)/4\pi] [h\omega_\lambda(n)/2C_\lambda(n)].$$

In the following, we restrict summations to the lowest quanta ($n = 1$), and two lowest multipolarities ($\lambda = 2, 3$). We apply the liquid-drop model (LDM) expressions for $\hbar\omega_\lambda$ and C_λ with the important modification, however, that the LDM mass parameters, D_λ , are scaled linearly to reproduce on the average the experimental systematics.¹¹ After adopting this prescription there is no free parameter.

The calculated σ_l distributions are given in Fig. 1. They are compared to the Bass-model smooth-cutoff distributions,

$$\sigma_{L-Bass}[\text{mb}] = \frac{10(2L+1)\pi\lambda^2}{1 + \exp[(L - L_{\max})/\Delta]},$$

where Δ is determined from requirement $\sigma_{\text{fu-Bass}} = \sum_L \sigma_{L-Bass}$. For symmetric reactions the partial-wave distributions are considerably broader than for asymmetric systems. The effect is particularly pronounced at the lowest energy, i.e., slightly above or below the barrier. In Table II the calculated cross sections are compared to the measured ones. At the highest energy the measured cross sections are always overestimated. This difference may be due to charged-particle evaporation. Statistical calculations predict that evaporation of charged particles, which should be negligible at the lowest energy ($\sim 5\%$), contribute roughly 20% at the highest energy. The calculated average angular momenta $\langle L \rangle_\nu$ which are also given in Table II agree, in all cases, with the measured values $\langle L_\gamma \rangle$ within the experimental errors.

By use of the theoretical σ_l distributions the relative neutron-evaporation cross sections have been calculated by the statistical model code PACE.¹² The $E1$ γ -ray

emission-strength function included the giant dipole resonance with position, shape, and strength which bring an excellent agreement with the observed γ spectrum between 2 and 20 MeV in the $^{16}\text{O} + ^{144}\text{Nd}$ reaction under the same experimental conditions.¹³ Contrary to Ref. 5 we did not use an elevated yrast line in our analysis. We have taken the experimental yrast line of ^{160}Er known up to spin $36\hbar$ (Ref. 3). Above this value, the theoretical yrast line was used. Our deformed Woods-Saxon-potential cranking-model calculations indicate that in $^{158-160}\text{Er}$ no superdeformed configurations occur up to $I \approx (60-70)\hbar$ while in ^{156}Er the superdeformation onset corresponds to $I \geq 40\hbar$. Therefore the influence of the superdeformation on the behavior of the compound nucleus studied in Ref. 5 cannot *a priori* be excluded.

The calculated ratios of the $3n$ - and $2n$ -channel cross sections are compared to the data in Table II. The agreement is good; in particular the calculations reproduce very well the suppression of the neutron emission observed in symmetric reactions. It should be emphasized that this result is obtained without the need to enhance⁶ the $E1$ γ -decay probability.

In conclusion, in heavy-ion-induced near-barrier reactions average γ -ray multiplicities of individual exit channels can no longer be explained by the sharp cut-off model when the masses of the target and projectile are comparable. As illustrated by calculations which take into account the ground-state zero-point vibrations, fusion partial-wave distributions can be dramatically modified and can extend to *very high partial waves*. This leads to pronounced effects in the decay of the compound system.

One of us (J.D.) wishes to acknowledge illuminating discussions with Dr. B. B. Back.

¹R. Bass, Nucl. Phys. **A231**, 45 (1974).

²R. A. Broglia, Nucl. Phys. **A409**, 163c (1983); C. H. Dasso, NORDITA Report No. Nordita-84/11, 1984 (to be published).

³J. Simpson *et al.*, Phys. Rev. Lett. **53**, 648 (1984); M. A. Riley *et al.*, Phys. Lett. **135B**, 275 (1984); T. Byrski *et al.*, Phys. Lett. **102B**, 235 (1981).

⁴D. Ward *et al.*, Nucl. Phys. **A397**, 161 (1983).

⁵W. Kühn *et al.*, Phys. Rev. Lett. **51**, 1858 (1983).

⁶C. Cabot *et al.*, Phys. Lett. **96B**, 55 (1980); C. Cabot *et al.*, to be published.

⁷R. M. Diamond and F. S. Stephens, Annu. Rev. Part. Sci. **30**, 85 (1980).

⁸J. Blocki *et al.*, Ann. Phys. (N.Y.) **105**, 427 (1977).

⁹H. Esbensen *et al.*, Phys. Rev. Lett. **41**, 296 (1978).

¹⁰C. M. Dasso *et al.*, Nucl. Phys. **A405**, 381 (1983).

¹¹A. Bohr and B. R. Mottelson, *Nuclear Structure* (Benjamin, Reading, 1975), Vol. 2, Figs. 6-28 and 29.

¹²A. Gavron, Phys. Rev. C **21**, 230 (1980).

¹³J. Barrette *et al.*, to be published.